Chapter 2
Piezoelectric Transducers Used for Piezoelectric Accelerometers with Integral Electronics

Keywords Piezoelectric transducer: bending mode; compression mode; equivalent electrical schematic; flexural mode; shear mode; transfer function • Piezoelectric elements: quartz; Lead Zirconate Titanate (PZT) • Piezoceramic • Pyroelectric effect

This chapter describes the piezoelectric (PE) transducers, the mechanical parts of piezoelectric accelerometers with integral electronics (IEPE). The function of the PE transducer in an IEPE accelerometer, its transfer function, equivalent electrical schematic, main electrical characteristics, construction, and types are described. Three basic types of PE transducers used in IEPE accelerometers, compression, shear, and flexural, their advantages and drawbacks are presented. Topics also include description of the piezoelectric (crystal) elements, the primary sensitive elements used in IEPE accelerometers. Two most popular piezoelectric element materials used in IEPE sensors, quartz and lead zirconate titanate (PZT) piezoceramic, their advantages and drawbacks are presented.

2.1 Function of a PE Transducer in an IEPE Accelerometer

The PE transducer is an IEPE accelerometer's mechanical part which transforms the input acceleration signal into an output charge electrical signal. The construction, size, and key electrical parameters of the PE transducer, such as charge and voltage sensitivities, capacitance, and resistance play an important role in the performance of an IEPE sensor. The integral electronics is comprised of a built-in FET-input charge or voltage amplifier which converts charge signal coming from the PE transducer into the output voltage signal. The amplifier transforms the PE

F. Levinzon, *Piezoelectric Accelerometers with Integral Electronics*,
DOI 10.1007/978-3-319-08078-9_2

transducer's high impedance into low output impedance allowing transmission of the voltage signal over long cable lengths.

There is a well-known conventional class of PE accelerometers using the PE transducer without electronics described in many literature sources [1–27]. This type of sensor is also called the Charge Mode PE accelerometer (or Charge Output PE accelerometer) in contrast to a Voltage Mode PE accelerometer (or Voltage Output PE accelerometer), which is the other name for the IEPE accelerometer. Design, characteristics, and construction of PE accelerometers are different in comparison with the PE transducers used in IEPE accelerometers. The PE transducers' function, construction, and characteristics are dictated by their operation as a mechanical part of an IEPE accelerometer. The PE transducer and the built-in FET-input charge or voltage amplifier should meet each other and have specific parameters described below.

2.2 Transfer Function of a PE Transducer

The basic structure and operation of a transducer can be modeled as a damped harmonic oscillator with mass *m,* spring constant *k*, and mechanical resistance *r* [16, 17]. Figure 2.1 shows the simplified schematic diagram of a PE transducer [16, 17].

This schematic can be described with the help of the classical second-order differential equation of motion for the output displacement signal z [16, 17, 28]:

$$m\frac{d^2z}{dt^2} + r\frac{dz}{dt} + kz = -m\frac{d^2y}{dt^2} \tag{2.1}$$

In (2.1), y is the input displacement signal. In the frequency domain, the input displacement signal is Y(f) and the response is Z(f) The solution for (2.1) for the output displacement signal spectral density |Z(f)| in $\mathrm{m}/\sqrt{\mathrm{Hz}}$ is given [28]:

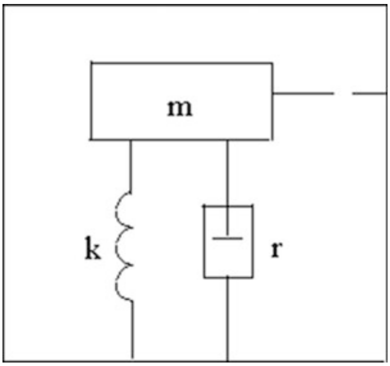

Fig. 2.1 Simplified schematic diagram of a PE transducer

$$|Z(f)| = \left(\frac{\omega}{\omega_n}\right)^2 |Y(f)|G(f), \tag{2.2}$$

where
$$G(f) = \frac{1}{\sqrt{\left[1-\left(\frac{\omega}{\omega_n}\right)^2\right]^2 + \left(\frac{\omega}{\omega_n}\right)^2 \frac{1}{Q^2}}}. \tag{2.3}$$

In (2.2), (2.3), $\omega = 2\pi f, \omega_n = 2\pi f_n, f_n$ is the resonant frequency:

$$\omega_n{}^2 = \frac{k}{m}, \tag{2.4}$$

and Q is the quality factor (factor of amplitude increase at resonance) of the harmonic oscillator:

$$Q = \frac{\omega_n m}{r}. \tag{2.5}$$

Since $\omega^2|Y(f)|$ is the magnitude of the input acceleration signal a_s measured in $\frac{\mathrm{m}}{\mathrm{s}^2\sqrt{\mathrm{Hz}}}$, the expression (2.2) can be rewritten

$$|Z(f)| = a_s|H(f)|, \tag{2.6}$$

where
$$|H(f)| = \frac{G(f)}{\omega_n{}^2}. \tag{2.7}$$

$H(f)$ is the transfer function of the PE transducer. For an IEPE accelerometer, the typical operating frequency range is restricted to $\omega < 0.3\omega_n$. Then, according to (2.3), $G(f) \approx 1$ and expressions (2.6) and (2.7) become

$$|Z(f)| = a_s\left(\frac{1}{\omega_n}\right)^2, \tag{2.8}$$

$$|H(f)| = \frac{1}{\omega_n{}^2}. \tag{2.9}$$

2.3 Equivalent Electrical Schematic of a PE Transducer and Its Main Electrical Characteristics

Simplified, but sufficient for IEPE accelerometer design purposes, the equivalent electrical schematic of a PE transducer can be presented as the voltage source electromotive force (EMF) e_{PE} and capacitance C_{PE} connected in series (see Fig. 2.2) [9]. Here e_{PE} and C_{PE} represent the output voltage of the open-circuit PE transducer and its electrical capacitance, respectively:

$$e_{PE} = a_s \cdot V_{PE}. \tag{2.10}$$

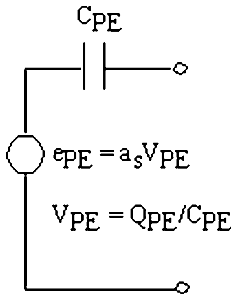

Fig. 2.2 Simplified electrical schematic of a PE transducer

In (2.10), a_s is the input acceleration and V_{PE} the PE transducer's voltage sensitivity typically measured in mV/g. V_{PE} has the following obvious relationship with the PE transducer's charge sensitivity Q_{PE} commonly measured in pC/g:

$$V_{PE} = \frac{Q_{PE}}{C_{PE}}. \tag{2.11}$$

In practice, using conventional units, (2.11) can be rewritten as

$$V_{PE}\left(\frac{\mathrm{mV}}{\mathrm{g}}\right) = \frac{Q_{PE}\left(\frac{\mathrm{pC}}{\mathrm{g}}\right)\cdot 1000}{C_{PE}(\mathrm{pF})}. \tag{2.12}$$

Q_{PE}, V_{PE}, and C_{PE} are the main electrical characteristics of the PE transducer which are needed for design of the IEPE accelerometer. As was shown in Chap. 1, Q_{PE} and V_{PE} are used for finding total sensitivities of a Charge Mode IEPE and Voltage Mode IEPE accelerometers, respectively. C_{PE} can affect the frequency response of a Charge Mode IEPE sensor and the total sensitivity of a Voltage Mode IEPE sensor. One more parameter, the PE transducer insulation resistance R_{PE} needs to be added to these characteristics. Since the PE transducer is connected in parallel with the input of the following FET- input amplifier, R_{PE} value can affect bias voltage provided for FET and, therefore, the output bias voltage of the whole sensor. To avoid influence of R_{PE} on the amplifier's bias, the R_{PE} value should meet the following requirement:

$$R_{PE} \gg R_{in} \tag{2.13}$$

where R_{in} is the input resistance of the amplifier. The requirement (2.13) must be provided over the entire operating temperature range of the sensor. In practice, it is sufficient to fulfill $R_{PE} \approx 10R_{in}$ for most cases. Typical value of R_{PE} in an IEPE accelerometer is $R_{PE} \geq 10^{10}\Omega$ ($\geq$10 GΩ).

2.4 Constructions of the PE Transducers Used in the IEPE Accelerometers

The PE transducers placed inside IEPE accelerometers have various construction designs dictated by the performance characteristics required for the sensors and the built-in FET-input charge or voltage amplifier used. There are three main PE transducer's construction designs used in IEPE accelerometers: compression mode, shear mode, and bending or flexural mode [1, 10, 11].

2.4.1 Compression Mode Design

The compression mode is the PE transducers' historically earliest design explained by its relatively simple structure. Figure 2.3 shows one of the compression mode design options called the Single-Ended Compression (SEC) [1] or Upright Compression Mode design [11].

In this design option, the piezoelectric (crystal) element is placed between a base and an inertial mass. Typically, the crystal element is pre-stressed with the help of the preload bolt which is torqued down to secure the mass to it. In some options, a mass and a crystal element are torqued on a central post [1]. The crystal element electrodes are connected with the charge or voltage amplifier board with the help of wires. The signal from the amplifier goes to the output connector. When acceleration is applied to the sensor, the mass creates force acting upon the crystal element resulting in a proportional electrical charge signal on its electrodes. In this construction, the crystal element creates charge in the same direction as the applied force. A larger mass produces more stress on the crystal element and, hence, the output signal has a larger value.

This design features a higher ruggedness, stiffness, and rigidity in comparison to other designs. As a result, it exhibits high resonant frequencies, resulting in wider

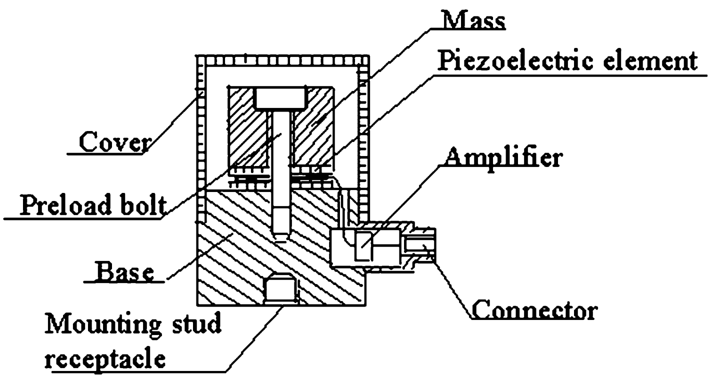

Fig. 2.3 Single-ended (upright) compression mode design of the IEPE accelerometer

frequency band. Also, this design typically can withstand high levels of vibration transients (shock level).

But, the compression structure has the following drawbacks. From Fig. 2.3 we can see that the piezoelectric element has good mechanical contact with mounting base. As a result, this design is sensitive to base bending (has more base strain sensitivity) and thermal transients (pyroelectric effect). The error in measured signal caused by those impacts can be large and, hence, can significantly reduce dynamic measurement range.

With the purpose to reduce the effects of base-coupled inputs, the isolated options of the compression mode are designed [1, 11]. The mechanical isolation of the crystal element from the mounting base is attained by implementing mechanical barriers between the crystal element and the mounting base. In one of these options called Isobase Compression design [1] or Inverted Compression design [11], the specially countered base creates a mechanical barrier. The other option called Isolated Compression design [11] uses an isolation washer combined with a hollowed-out mass acting as a thermal insulation barrier [11].

Even though the mechanical enhancements mentioned above improve the construction shown in Fig. 2.3 resulting in more stable performance, the compression mode design is seldom used in modern IEPE accelerometers.

2.4.2 Shear Mode Design

This is the most popular design used in IEPE accelerometers [1–5]. This preference is explained by its advantages in comparison to other design options. Figure 2.4 shows an example of the Shear Mode design options called an Annular Shear Mode IEPE accelerometer [1, 2, 11].

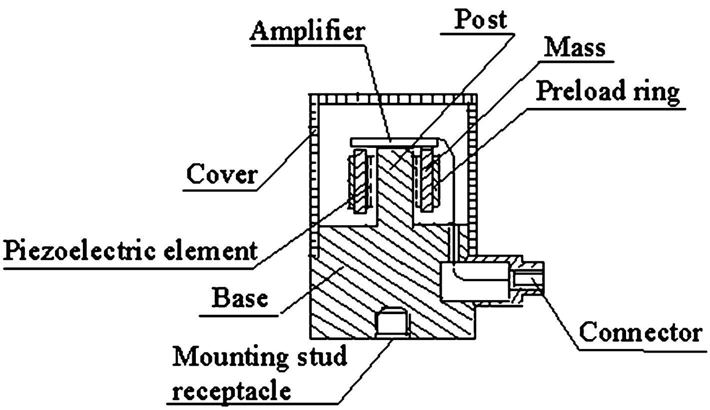

Fig. 2.4 An example of the Annular Shear Mode design of an IEPE accelerometer

In Fig. 2.4, the mass is attached to the periphery of the crystal element which, in turn, is secured to the central post. With the purpose to provide a stiff, rigid, linear structure with wide frequency band, a compression ring creates a preload force to the mass-crystal assembly. When acceleration is applied to the sensor, the mass causes a shear force to be applied to the crystal element. In this construction, the crystal element generates charge in the direction perpendicular to the applied force.

There are several options for this design used in practice. Among them are the Annular Shear design shown in Fig. 2.4 and Isoshear design using a stack of flat crystal elements attached to the central post by a mounting bolt [1].

This structure offers high charge output and provides good mechanical isolation of the sensing element from the base. As a result, the Shear Mode design offers the high value of sensor's sensitivity and the best protection against base bending and thermal transients (pyroelectric) effects. The Isoshear design allows the use of many crystal elements and passive temperature compensators to provide a broad range of sensitivities, stable performance over wide temperature interval, and low noise floor [1, 2]. Figures 2.5 and 2.6 show photographs of two recently designed IEPE accelerometers operating in the Annular Shear Mode [29, 30]. The first one represents a single axis two wire output sensor family featuring 100, 500, and

Fig. 2.5 Photograph of the single axis 1 V/g Annular Shear Mode IEPE accelerometer

Fig. 2.6 Photograph of the triaxial 1 V/g Annular Shear Mode IEPE accelerometer

Fig. 2.7 Photograph of the Shear Mode IEPE accelerometer with the center-hole design

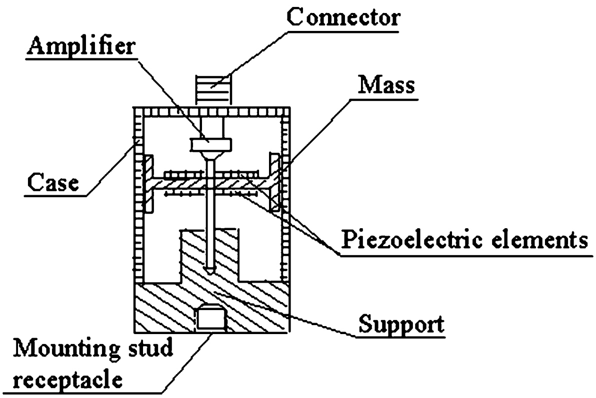

Fig. 2.8 An example of construction of the Flexural (Bending) Mode IEPE accelerometer

1,000 mV/g sensitivity options [29]. The second one is a triaxial 4-pin connector IEPE accelerometer representing the sensor family having the 500 and 1,000 mV/g sensitivity options [30].

Some of the Shear Mode constructions have the center-hole mounting option allowing the user to precisely orient the connector and cable when installing accelerometers in close quarters [1]. Figure 2.7 shows the photograph of one such accelerometer featuring wide bandwidth (up to 20 kHz at level of ±10 %) and light weight (1.8 g) [31].

2.4.3 Flexural or Bending Mode Design

The Flexural or Bending Mode design of an IEPE accelerometer is comprised of piezoelectric elements attached to the seismic mass having the shape of a beam [1, 10, 11]. In practice, this beam generally has a double cantilever form. Figure 2.8 shows an example of this construction [1, 11].

The accelerometer has a cylindrical shape and is comprised of PE elements, mass, support, amplifier, and case. The one piece mass consists of a cylindrical and cross-beam sections. The piezoelectric elements are bonded to the cross-beam section in its center. Vibration axis is the same as the cylinder axis. With acceleration signal in this direction, the mass bending causes the PE elements to generate electrical signal. The signal is amplified by the amplifier and exits at the connector. This construction features high sensitivity, low resonant frequency, good thermal stability (low pyroelectric effect), and low noise floor [1, 10, 11, 32, 33]. The flexural design is typical for so called IEPE seismic sensors used for applications required the measurement of low-frequency and low-level acceleration signals. Figures 2.9 and 2.10 show photographs of two ultra-low noise IEPE seismic sensors having the flexural mode construction [32, 33]. The first one features sensitivity

Fig. 2.9 Ultra-low noise 10 V/g IEPE flexural mode seismic accelerometer

Fig. 2.10 Ultra-low noise 10 V/g IEPE compact flexural mode seismic accelerometer

Table 2.1 Comparison between compression, shear, and flexural mode designs

Compression IEPE design		Shear IEPE design		Flexural IEPE design	
Advantages	Drawbacks	Advantages	Drawbacks	Advantages	Drawbacks
High ruggedness, stiffness, and rigidity	High base strain sensitivity	Small base strain sensitivity	Not high enough resonant frequency in some designs	Best sensitivity-to-mass ratio	Low resonant frequency
High resonant frequencies	High sensitivity to pyroelectric effect	Small sensitivity to pyroelectric effect		Small sensitivity to pyroelectric effect	Fragile construction
High shock level	Higher noise floor	Higher sensitivity-to-mass ratio than compression mode		Low noise floor	
	Lower sensitivity-to-mass ratio than other options	Stable performance over wide temperature range			

10 V/g and a noise floor estimated at $40\,\text{ng}\sqrt{\text{Hz}}$ at frequency 1 Hz and $3\,\text{ng}\sqrt{\text{Hz}}$ at frequency 100 Hz [32]. This sensor has a cylindrical shape with a diameter of 65 mm, a height of 56 mm, and a weight of 770 g. The second one is also an ultra-low noise sensor with the same sensitivity, but it is compact having cylindrical shape with a diameter of 29 mm, a height of 37 mm, and a weight of 170 g [33]. This sensor has a slightly higher noise floor, specifically, $90\,\text{ng}\sqrt{\text{Hz}}$ at frequency 1 Hz and $10\,\text{ng}\sqrt{\text{Hz}}$ at frequency 100 Hz. More detailed description of these sensors will be made in the following chapters.

2.4.4 Comparison Between Compression, Shear, and Flexural Mode Designs

Table 2.1 shows advantages and drawbacks of these three designs.

2.5 Piezoelectric Elements Used in the IEPE Accelerometers

Piezoelectric PE (crystal) elements are the primary sensing elements which produce electrical signal when stressed by force. The selection of the PE element materials plays a critical role in the sensors' performance.

2.5.1 Quartz Piezoelectric Element

Natural PE crystals, such as quartz and tourmaline, have high levels of Curie temperatures, the temperatures at which they lose their piezoelectric properties [20]. Specifically, quartz allows PE sensors to operate at temperatures as high as 315 °C [11]. In practice, PE accelerometers with quartz have maximum temperature not more than 260 °C due to twinning of the quartz crystal element. But the temperature limit for electronics does not allow using quartz potential ability in IEPE sensors.

Quartz crystal element offers stable operation over a wide temperature range and exhibits very low pyroelectric output [11, 20]. In addition, quartz exhibits a low value of the charge sensitivity, a small value of the electrical capacitance C_{PE}, and a high value of the voltage sensitivity V_{PE}. Typically, the single quartz crystal element has a capacitance value of less than 10 pF. A small value of C_{PE} and a high value of V_{PE} result in choosing the voltage amplifier as the preferable option for the PE transducer with quartz. This is because, if the charge amplifier is used, it would have, at such C_{PE} values, a very small feedback capacitance C_f comparable with the hybrid circuit's strays. That is why, in practice, the Voltage Mode IEPE is the typical type of sensor when the PE transducer comprises the quartz PE element.

With the purpose to provide good parameters required for the sensor, such as sensitivity at least 10 mV/g, frequency response with deviation of ≤5 % at frequency 1 Hz, and temperature range up to 125–130 °C, the voltage amplifier should have high value of input resistance R_{in} and small value of input capacitance C1 at such small C_{PE} values. High value of R_{in} can limit the temperature range of the sensor. As a result, tradeoffs in performance of the accelerometers for different applications are considered to optimize value of R_{in}. Since quartz has low charge sensitivity and low value of electrical capacitance, it cannot be used for design of the high sensitivity and low-noise IEPE accelerometers. The man-made ferroelectric materials with artificial polarization such as PZT piezoceramic are more appropriate for such IEPE sensors.

2.5.2 Lead Zirconate Titanate Piezoceramic Element

Ferroelectric ceramic materials such as PZT piezoceramic are known for their very high sensitivities and possibility providing extended frequency range, smaller noise, and smaller size when compared to the equivalent output of a natural crystals such as quartz or tourmaline [1–3, 20]. That is why PZT piezoceramic is widely used in the IEPE sensors. Table 2.2 shows typical charge output per unit force for quartz, PZT, and tourmaline.

Ferroelectric ceramic materials require polarization before use. The polarization process known as "poling" includes applying a high voltage to the material to align polar regions within the ceramic element [7].

In principle, the crystal elements made of PZT are able to operate at temperatures as high as 288 °C [20, 34]. But again, as in the case with quartz, integral electronics temperature limitation does not allow reaching such temperatures in the current IEPE sensors. The maximum temperature attained in the existing IEPE accelerometers with the PZT crystal elements and the FET-input amplifiers built using the silicon-based technology is 163–185 °C [35–41]. The IEPE accelerometers comprising the silicon-on-insulator (SOI) FET-input amplifiers have maximum operating temperature 225 °C at present.

Table 2.2 Comparison between different materials in charge output per unit force

		Quartz	PZT	Tourmaline
Charge output per unit force, pC/N	Shear mode	4	460	3.8
	Compression mode	2.2	350	1.9

Table 2.3 Comparison between IEPE sensors using PZT ceramic and quartz elements

IEPE sensors using PZT piezoceramic		IEPE sensors using a Quartz element	
Advantages	Drawbacks	Advantages	Drawbacks
Higher values of sensitivities	Higher sensitivity to pyroeffect	Less deviation in sensitivity over temperature range	Less values of sensitivities
Wider frequency range	More deviation in sensitivity over temperature range	More potential maximum operating temperature	Narrower frequency range
Lower noise	Presence of a slope of 2.5 % per decade in amplitude response in the Charge Mode IEPE sensors	Flat amplitude response (absence of slope of 2.5 % per decade)	Higher noise
Smaller size			Bigger size

2.5.3 Comparison Between IEPE Sensors Using PZT Piezoceramic and Quartz Sensitive Elements

Table 2.3 summaries comparison between IEPE sensors using PZT piezoceramic and quartz element.

2.5.4 The Pyroelectric Effect

The pyroelectric effect is generation of charge on the surface of a piezoelectric element when temperature gradients occur across the element [7]. This charge signal is mostly observed at low frequencies, typically below 10 Hz. The magnitude of the pyroelectric output depends on material of the crystal element and construction of the PE transducer. The piezoelectric element made of quartz lacks the pyroelectric effect. As mentioned above, the compression mode accelerometers can produce more pyroelectic output compared to the shear and flexural mode sensors. Since the pyroelectric output is a low frequency event, it can be filtered out by high-pass-filter (HPF) used in the electronics. However, if the low frequency spectrum of the acceleration signal is to be measured, it is important to know how sensitive to pyroelectricity the various crystal materials and constructions of the PE transducer are.

References

1. (2008) Dynamic test handbook. Shock vibration pressure. Meggitt, Endevco, San Juan Capistrano, CA. https://www.endevco.com/new-2008-endevco-dynamic-test-handbook-provides-complete-resource-for-frequently-needed-data/
2. (2012) Test and measurement product catalog. Meggitt Sensing Systems, Irvine, CA. https://www.endevco.com/resources/catalog/

3. (2011) Test & measurement, sensors & instrumentation catalog. PCB Piezotronics Corp., Depew, NY. http://www.pcb.com/FlipBookInteractive.aspx#.UsWRhqTxuUk
4. Handbook of piezoelectric accelerometers. Bruel & Kear, http://www.bksv.com/doc/bb0694.pdf
5. (2011) Dytran piezoelectric and DC MEMS sensors for measurement and monitoring, Product catalog . Dytran Instruments, Inc. Chatsworth, CA, http://catalog.dytran.com/
6. Wilson JS (2005) Sensor technology handbook. Newnes and Elsevier, Amsterdam. ISBN 0-7506-7729-5
7. Webster JG (1998) The measurement, instrumentation and sensors handbook. CRC, Boca Raton, FL
8. Tustin W (2005) Random vibration & shock testing. Equipment Reliability Institute, Santa Barbara, CA
9. Walter PL (2001) The handbook of dynamic force, pressure and acceleration measurement. Meggitt, Endevco, San Juan Capistrano, CA. http://www.amazon.com/handbook-dynamic-pressure-acceleration-measurement/dp/0971337004
10. Weber M (2013) Accelerometer designs. Metra Mess- und Frequenztechnik in Radebeul e.K. http://www.new.mmf.de/accelerometer_designs.htm
11. Function of piezoelectric accelerometers. PCB piezotronics. http://www.pcb.com/TechSupport/Tech_Accel
12. Merhav S (1996) Aerospace sensor systems and applications. Springer, New York
13. (2009) Practical understanding of key accelerometer specifications. Technical paper 328, Meggitt, Endevco Corp. https://www.endevco.com/download-center/
14. Kulwanoski G, Schnellinger J (2004) The principles of piezoelectric accelerometers. Kistler Instrument Corp. Sensors Magazine Online. http://www.sensorsmag.com/articles/0204/27/main.shtml
15. Isotron and charge mode piezoelectric accelerometers, pros and cons. Technical paper 320, Meggitt, Endevco Corp. https://www.endevco.com/download-center/
16. Gabrielson TB (1993) Mechanical-thermal noise in micromachined acoustic and vibration sensors. IEEE Trans Electron Devices 40(5):903–909
17. Longoria RG (2000) Note on accelerometers, The University of Texas at Austin, http://www.me.utexas.edu/~me244L/labs/motion/accelerometers.pdf
18. Wlodkowski PA et al (2001) The development of high-sensitivity, low-noise accelerometers utilizing single crystal piezoelectric materials. Sens Actuators 90:125–131
19. Aszkler C (2005) The principles of acceleration, shock, and vibration sensors. Sensors online magazine. http://archives.sensorsmag.com/articles/0505/14/main.shtml
20. Mattingly M (2008) Aerospace accelerometers. Quality Magazine, http://www.qualitymag.com/articles/89157-aerospace-accelerometers
21. Vives AA (ed) (2008) Piezoelectric transducers and applications, 2nd edn. Springer, Heidelberg
22. Steinem C, Janshoff A (eds) (2007) Piezoelectric sensors. Springer, Heidelberg
23. Moheimani SOR, Fleming AJ (2006) Piezoelectric transducers for vibration control and damping. Springer, Heidelberg
24. Tichy J, Erhart J, Kittinger E, Privratska J (2010) Fundamentals of piezoelectric sensorics. Springer, Heidelberg
25. Jalili N (2010) Piezoelectric-based vibration control. Springer, Heidelberg
26. Weber M (2013) Characteristics. Metra Mess- und Frequenztechnik in Radebeul e.K. http://www.new.mmf.de/characteristics.htm#frequ_resp
27. Lent B (2009) Simple steps to selecting the right accelerometer. Sensors online magazine. http://www.sensorsmag.com/sensors/content/printContentPopup.jsf?id = 586549
28. Acceleration measurements with piezo-electric accelerometers. http://stuff.mit.edu/afs/athena/course/13/13.80/www/handouts/Accelerometer.pdf
29. Isotron® accelerometer Model 43A. Meggitt Sensing Systems, Irvine, CA. https://www.endevco.com/wp-content/uploads/43A1.pdf

30. Isotron® accelerometer Model 45A. Meggitt Sensing Systems, Irvine, CA. https://www.endevco.com/wp-content/uploads/45A9.pdf
31. Model 7250A -2,-10 Isotron® accelerometer. Meggitt Sensing Systems, Irvine, CA. https://www.endevco.com/datasheets/7250A.pdf
32. (2009) Model 86 seismic accelerometer. Meggitt Sensing Systems, Irvine, CA. https://www.endevco.com/datasheets/86.pdf
33. Model 87 seismic accelerometer. Meggitt Sensing Systems, Irvine, CA. https://www.endevco.com/datasheets/87.pdf
34. Model 7703A -50,-100 piezoelectric accelerometer. Meggitt Sensing Systems, Irvine, CA. https://www.endevco.com/datasheets/7703A.pdf
35. Isotron® accelerometer Model 65HT, Specification Sheet. Meggitt Sensing Systems, Irvine, CA. https://www.endevco.com/wp-content/uploads/65ht6.pdf
36. Model 67 Isotron® accelerometer (2012). Meggitt Sensing Systems, Irvine, CA. https://www.endevco.com/datasheets/67.pdf
37. Triaxial CCLD accelerometer types 4527 and 4527-001. Product Data. B&K. http://www.specman.pt/4527.pdf
38. 4526—CCLD accelerometer. Specifications. http://www.bksv.com/Products/transducers/vibration/accelerometers/accelerometers/4526?tab=specifications
39. DJB Instruments, Piezo-Electric Accelerometers—A/123/S. http://www.djbinstruments.com/products/piezo-electric-accelerome ters/mono-axial-integral-electronics/a123s
40. DJB instruments, piezo-electric accelerometers—A/124/E. http://www.djbinstruments.com/products/piezo-electric-accelerometers/mono-axial-integral-electronics/a124e
41. PCB piezotronics, model: 356A15. Product specification. http://www.pcb.com/Products.aspx?m=356A15

Springer

http://www.springer.com/978-3-319-08077-2

Piezoelectric Accelerometers with Integral Electronics
Levinzon, F.
2015, XV, 169 p. 99 illus., 37 illus. in color., Hardcover
ISBN: 978-3-319-08077-2